

Hard thermal loops in the real-time formalism

Simon Caron-Huot

McGill University, 3600 rue University, Montréal QC H3A 2T8, Canada

E-mail: scaronhuot@physics.mcgill.ca

ABSTRACT: We present a systematic discussion of Braaten and Pisarski's hard thermal loop (HTL) effective theory within the framework of the real-time (Schwinger-Keldysh) formalism. As is well known, the standard imaginary-time HTL amplitudes for hot gauge theory express the polarization of a medium made out of nonabelian charged point-particles; we show that the complete real-time HTL theory includes, in addition, a second set of amplitudes which account for Gaussian fluctuations in the charge distributions, but nothing else. We give a concise set of graphical rules which generate both set of functions, and discuss its relation to classical plasma physics.

KEYWORDS: Hard thermal loops, real-time formalism, quark-gluon plasma.

1. Introduction

It is a theoretically interesting problem to compute the higher-order perturbative corrections received by physical observables in the quark-gluon plasma, especially in view of the present experimental program at RHIC [1] and of the future LHC heavy ion program. In particular, one would like to understand theoretically what the regime of validity of perturbation theory is, for various observables of interest, at least within the setup of a locally thermalized plasma.

Theoretical studies of the thermodynamic pressure, which is a quantity naturally accessible to Euclidean space techniques, have revealed a poor convergence of the perturbative series unless the strong coupling constant assumes unrealistically small values, $\alpha_s \lesssim 0.1$. In [2] this behavior was attributed to self-interactions of soft, gT scale, gauge fields ($g \equiv \sqrt{4\pi\alpha_s}$). Little is presently known about the corrections received by *dynamical* quantities, in particular those which are leading-order sensitive to the gT scale, such as photon production rates [3–6], jet energy loss [6, 7], heavy quark energy loss [8, 9] and transport coefficients (such as shear viscosity) [10]. These quantities all are leading-order sensitive to the gT scale, in the sense that they would be logarithmically infrared divergent were the screening effects which arise at this scale not properly resummed, and are “dynamical” in the sense that they describe real-time physics, making their extraction difficult from Euclidean space correlators (and thus from lattice data).

The plasma effects which arise at the gT scale are usually resummed, in a gauge invariant way, by means of Braaten and Pisarski’s hard thermal loop (HTL) effective theory [11]. This effective theory incorporates, to leading order in g , the effects from the scale T on the scale gT , in terms of (nonlocal) effective propagators and vertices. These ingredients can be used to build a loop expansion, which, so long as only the soft scale gT enters a problem, is an expansion into powers of g . Thus, since the above-listed dynamical quantities are leading-order sensitive to the gT scale, one expects them to receive potentially large $\mathcal{O}(g)$ corrections from soft loops in the HTL theory.

Until recently, there had been no calculation of the $\mathcal{O}(g)$ corrections received by *any* of these quantities. We believe there is a certain technical advantage in performing such calculations directly in Minkowski space, using real-time (Schwinger-Keldysh) techniques; however to the best of our knowledge a systematic discussion of the HTL theory within this formalism is presently lacking from the literature. In this paper we provide just such a discussion. We have recently applied the theory we present here to a next-to-leading order calculation of nonrelativistic heavy quark diffusion [12].

This paper is organized as follows. In section 2 we briefly recall the rules of the real-time formalism, in particular within the so-called Keldysh (“ r/a ”) basis. In section 3 we show, by a power-counting argument, that the HTL effective theory takes on an especially simple form in this basis: the only HTL amplitudes (with external gauge bosons) carry at most two a Keldysh indices, though arbitrarily many r indices. In section 4 we compute these amplitudes, which have a simple and physically transparent form, and give their generating functional.

A convenient set of effective graphical rules which generate the real-time HTL theory is given in section 5; these rules are essentially a graphical realization of the nonabelian Vlasov equations (including, as well, Gaussian fluctuations in the particle distribution functions.) We discuss the relationships between our results and previous work, and with the classical plasma physics of a gas of point-like nonabelian charges, in section 6. Since our method of analysis appears to shed little light on the structure of real-time perturbation theory when soft fermions are involved, we leave the analysis of fermionic HTLs to future work.

2. The real-time formalism

The real-time formalism allows the description of the dynamical evolution of expectation values within some initial state or density matrix (as opposed to “in-out” transition amplitudes). The formalism is characterized by a doubling of the degrees of freedom: in addition to the usual “ ϕ_1 ” fields which implement forward time evolution, one should path-integrate over a second set of fields, “ ϕ_2 ”, which implement time evolution backward in time to some initial time. We work in the so-called Keldysh r/a basis, obtained via the change of basis $\phi_r = \frac{1}{2}(\phi_1 + \phi_2)$ and $\phi_a = \phi_1 - \phi_2$, and let the initial time at which the system’s density matrix is defined go to $-\infty$. For a review we refer the reader to [13]¹.

Here we merely recall the rules of perturbation theory in this context. In thermal equilibrium the propagator is a 2×2 matrix, which takes the form

$$G \equiv \begin{pmatrix} G_{rr} & G_{ra} \\ G_{ar} & G_{aa} \end{pmatrix} = \begin{pmatrix} (G_R - G_A) \left(\frac{1}{2} \pm n(p^0) \right) & G_R \\ G_A & 0 \end{pmatrix}, \quad (2.1)$$

where $n(p^0) \equiv 1/(e^{p^0/T} \mp 1)$ denote the standard Bose-Einstein and Fermi-Dirac distributions, for bosons and fermions respectively. For a free scalar field, the retarded propagator G_R would be given as² $G_R(P) = -i/(P^2 + m^2 - i\epsilon p^0)$ in Fourier space. The general form (2.1) holds nonperturbatively: the propagator is completely determined by G_R . The chief reason for using the r/a basis in this work is that Bose-Einstein distributions, which play a key role when treating soft physics, appear in only one matrix element of the propagator, and are therefore most conveniently managed.

To perform perturbative calculations, one must sum over the r/a assignments for all internal legs in Feynman diagrams, subject to the restriction that the vertices carry an odd number of a indices. The vertices having one a index coincide with the standard zero-temperature ones, and those having three a indices are smaller by a factor 1/4. External r and a fields in correlation functions carry distinct physical meaning: since the difference field ϕ_a is analogous to an interaction term which would be added to the Hamiltonian, general correlators of a and r fields may be understood in terms of the (retarded) nonlinear response

¹Our r/a fields correspond to the 1/2 fields of the “physical representation” used by these authors.

²Our metric is $(-+++)$, and following finite temperature conventions, we capitalize four-vectors but write their components as lowercase.

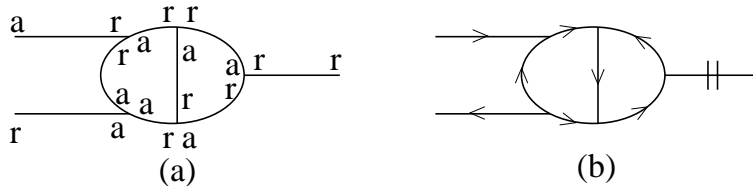


Figure 1: Example of a Feynman diagram in the r/a formalism, with (a) explicit marking of r/a indices and (b) our graphical notation. The propagators which carry arrows are retarded, and the cut propagator is an rr propagator.

induced by the a fields on some correlator of r fields [13]. Correlators in which the a field has the largest time argument vanish, $\phi_a(t) \rightarrow 0$ as $t \rightarrow \infty$.

We graphically represent Feynman diagrams in the r/a formalism by drawing incoming arrows on r fields which enter interaction vertices, and outgoing arrows on a fields. With this notation, retarded and advanced propagators bear a single arrow, which points in the direction of the flow of time. An rr propagator carries two outgoing arrows, which we separate by a “cut”: we think of the cut as a place where the time flow can start. Sometimes we will omit to draw the arrows on these propagators, which should create no confusion. The (tree-level) interaction vertices all have an odd number of outgoing arrows. Our graphical notation is illustrated in Fig. 1. Incidentally, this particular diagram yields zero, because it contains a closed loop of retarded propagators.

3. Power counting

We consider (amputated) vertex functions in which all of the external legs are soft gauge bosons; by soft we mean $P \sim gT$ and by hard we mean $P \sim T$, for all components of P . We recall that vertex functions having only one Keldysh a index, often called “fully retarded functions”, correspond to a direct analytic continuation of the Euclidean vertex functions [14], and that these HTL amplitudes are of parametric size $g^2 T^{4-n}$, where n is the number of external legs [11, 15]. Amputated vertex functions with no external a index vanish, because correlation functions involving only a fields vanish. There are no HTL amplitudes involving external ghost fields [11], at least within the classes of covariant and Coulomb gauges, so we will not consider diagrams with external ghost lines. We now show that loop amplitudes with n external legs, n_a of which bearing Keldysh a indices, can only compete with the above-mentioned HTL amplitudes if they are of parametric size $g^{3-n_a} T^{4-n}$. Then we show that no hard loop can be parametrically larger than gT^{4-n} , implying that vertex functions with $n_a \geq 3$ are not part of the HTL theory. We also show that the soft contribution to one-loop amplitudes behaves like $g^{4-n_a} T^{4-n}$ and produces subleading effects relative to the HTLs, although vertex functions with $n_a \geq 3$ are soft-dominated, not hard-dominated. The key ingredients entering our power-counting are summarized in Table 1.

Vertex functions with more external Keldysh a indices, when they appear within Feynman diagrams, tend to be suppressed due to the (absence of) Bose-Einstein factors on the propagators connecting to them. To see this, we note that when a vertex function carries an a index, the Keldysh index on the remote side of the propagator connecting to it must necessarily be an r index, because of the absence of an aa propagator. There thus automatically exists a corresponding diagram in which the a index on the vertex function is replaced with an r , and the ar propagator replaced with an rr propagator; since for soft external momenta the latter propagator is larger by one Bose-Einstein factor $T/p^0 \sim 1/g$, we see that the original vertex function will only compete with the latter if it is parametrically larger by one factor $1/g$. By induction this proves our first claim: amputated vertex functions with n external legs, n_a of which carrying a indices, will only compete with the HTL amplitudes with one external a index if they are of parametric size $g^{3-n_a}T^{4-n}$.

Ingredient	Parametric strength
Soft (bosonic) retarded propagator	$1/g^2T^2$
Soft (bosonic) rr propagator	$1/g^3T^2$
Hard, near light-like propagator	$1/gT^2$
Hard three-point vertex	gT
Soft three-point vertex	g^2T
d^4Q for hard, near light-like Q	gT^4
d^4Q for soft Q	$(gT)^4$

Table 1: Ingredients which enter our power-counting.

We now show that it is impossible for a hard loop with n soft external (gauge boson) legs to be parametrically larger than gT^{4-n} . Indeed, let us consider a bosonic loop diagram (the conclusion being unchanged for fermionic loops), having n three-point vertices and no four-point vertices (it can be shown that the latter get suppressed in general.) The dominant contribution from the region of hard loop momentum $Q \sim T$ arises when Q is within gT of the light cone, in which case each propagator contributes a large $\sim 1/gT^2$ factor. This is because, for generic soft external momenta, no two hard propagators can simultaneously become closer to the light cone than gT , and parametrically nothing special happens when only one propagator becomes arbitrarily close to the light-cone (because of the corresponding measure suppression); this region maximizes the number of simultaneously large propagators. The estimate $1/gT^2$ for hard, near light-like, propagators is independent on the hard propagator being retarded or cut³. The restriction of the integration measure d^4Q to the hard, near light-like region produces a factor of gT^4 , and counting the n three-point interaction

³Enforcing the mass-shell condition on some hard propagators, when they are G_{rr} propagators, can force linear combinations of the external momenta to be spacelike, but this does not represent a *parametric* suppression of the phase space of the soft external momenta. What we are saying is that, for $Q = R + P$ with $R^2 = 0$ and P soft, $Q^2 \approx 2R \cdot P$, it is fair to treat $1/(2R \cdot P \pm i\epsilon r^0)$ and $\delta(2R \cdot P)$ as parametrically equivalent, $\sim 1/gT^2$.

vertices each as gT , we find that a hard loop with n external legs can behave at most like gT^{4-n} parametrically. Actually a cancellation occurs when $n_a = 1$ so these functions behave like g^2T^{4-n} , but we will see in the next section that no such cancellation occurs when $n_a = 2$. Together with the last paragraph, this shows that *hard* loops with $n_a \geq 3$, when appearing inside full diagrams, have subleading effects relative to those with $n_a = 1, 2$.

What about soft loops? Using the rules of the r/a formalism, it can be shown that loop diagrams with n_a external a indices can contain up to n_a internal cut (rr) propagators. For bosonic loops, the presence of n_a Bose-Einstein functions suggests that diagrams with n_a large should be soft-dominated, not hard-dominated. This indeed happens: in the soft region, a (bosonic) retarded propagator should be estimated as parametrically $1/g^2T^2$, a cut propagator estimated as $1/g^3T^2$, a three-point interaction vertex treated as g^2T , and the integration measure treated as $(gT)^4$. Adding up, we find that the soft loop contribution to a bosonic loop diagram is parametrically $g^{4-n_a}T^{4-m}$. Since soft loops should actually be evaluated using effective HTL-resummed propagators and vertices, which are quite complicated expressions, we do not expect parametric cancellations to occur.

For $n_a = 1, 2$ the soft contribution is down by exactly one power of g relative to the hard contribution: these diagrams are truly hard-dominated and deserve to be called “hard thermal loops.” Hard loops with arbitrary external r/a indices were considered in [16], in which it was found that due to a cancellation hard loops with $n_a = 3$ were of parametric order g^2T^{4-m} (however these authors did not recognize that hard loops with $n_a \geq 3$ only had subleading importance in actual calculations). Thus we see that hard loops with $n_a \geq 3$ not only have subleading effects, they are also incorrect: the corresponding diagrams are *soft*-dominated, not hard-dominated. However this poses no problem to power-counting: when present inside diagrams, soft loops having arbitrary numbers of external a indices all contribute at the same order as the soft contribution to the $n_a = 1$ loops, e.g. are down by $\mathcal{O}(g)$ relative to the HTL contribution. Essentially what happens is that by modifying the external r/a indices on a soft loop, one is merely transferring the Bose-Einstein factors back and forth between the propagators outside and inside the loop.

The HTL amplitudes account for the dominant effects from hard particles on soft gauge fields, and together with the tree interactions vertices (which are of the same order), they can be used to set up an effective theory which contains only the gT scale. We believe that the loop expansion within this theory, in the real-time formalism, proceeds in a way entirely similar to that in the imaginary-time formalism [11]: as long as only the scale gT contributes, each additional loop is suppressed by one power of g ⁴. In general, in a theory with only one physical scale, one would expect the loop expansion to be an expansion into powers of g^2 ; in the imaginary-time formalism one gets an expansion into powers of g , because each additional soft loop can introduce one (and only one) additional Bose-Einstein factor. Within the real-

⁴Of course, in practice such an expansion is not expected to hold up to arbitrarily high order, since other scales should eventually enter (associated e.g. with some mean free path, or with nonperturbative, infrared physics). However, the appearance of a new physical scale would be signaled by a divergence in the HTL effective theory, because it contains only one scale.

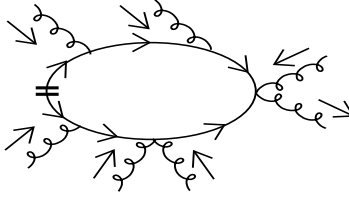


Figure 2: The most general one-loop diagram with one external a index (the outgoing arrow), but many r indices: all such diagrams only have one cut propagator. The arrow flow corresponds to time flow; we do not specify the nature of the particle running in the loop.

time formalism, this well-known statement must be modified to the claim that each additional loop introduces one (and only one) additional Bose-Einstein factor *or* HTL vertex functions with two external a indices. The latter vertices may be regarded as secretly containing one Bose-Einstein factor, since they are larger by a factor $1/g$. We will not embark here into a general proof of this claim, which would be easy to give using the effective Feynman rules we present in section 5; we simply remark that it would be quite surprising for a systematic loop expansion to hold within one formalism, and not within another.

4. Calculation of the hard thermal loops

4.1 HTLs with one a index

The gluonic hard thermal loops having only one external Keldysh a index, often called “fully retarded functions”, can be obtained via a direct analytic continuation of the well-known Euclidean ones [11] [15], and thus do not need to be independently recomputed within the real-time formalism. Nevertheless, we think it is instructive to briefly describe the Feynman diagrams which contribute to them, and how, following [19, 20] they can be evaluated using a simple kinetic theory of point-like particles.

The most general one-loop Feynman diagram with one external a index, but arbitrarily many r indices, is illustrated in Fig. 2. All of these diagrams contain only one cut (rr) propagator, which occurs at the smallest time in the diagram. In terms of our graphical notation, this structure can be tracked down to the fact that inserting an external r field (incoming arrow) onto a diagram (involving only bare interaction vertices), be it onto an existing vertex or onto a propagator, never modifies its arrow flow. Physically, this structure means that these functions represent the nonlinear response of the expectation value of the gauge current (at the a leg) due to a background field (the r legs): the Feynman diagrams mimic the obvious quantum-mechanical procedure of starting with an initial one-particle density matrix (here, the “cut”), evolving it under a background field, and taking the expectation value of the current at late times.

In [19] the problem of calculating the induced current in a soft background gauge field

(mean field) was considered, and reduced to kinetic theory:

$$J_{\text{ind}}^{\mu a}(X) = \sum_{\text{DOF}} g \int \frac{d^3 p}{(2\pi)^3} v^\mu n^a(X, \mathbf{p}), \quad (4.1)$$

$$v \cdot D n^a(X, \mathbf{p}) = g \text{Tr}_r \left[t_r^a t_r^b \right] dv^i E^{ib}(X) \frac{-dn(p)}{dp}, \quad (4.2)$$

where $v^\mu = (1, \mathbf{p}/p)$ represents the four-velocity of a hard particle and n denote the standard Bose-Einstein or Fermi-Dirac distributions. The second equation, to be solved with retarded boundary conditions, determines the color-adjoint disturbance n^a . The concept of point-like particles originates from the separation of scales $gT \ll T$, between the momenta of the external gauge field and that of the typical particles which contribute to the induced current: the hard particles feel the external field as if they were point particles. The degree of freedom count in (4.1) is: two bosonic degrees of freedom for the gauge/ghost system, four fermionic degrees of freedom for Dirac fermions, and two bosonic degrees of freedom for complex scalar fields; the form of the resulting equations is the same for all of these particles, and is gauge-fixing independent [11]. A collision term is not included in (4.2) because collisions are only relevant over $1/g^2 T$ time scales; for a more ample discussion we refer to the review [21].

Solving for the induced current (4.1)-(4.2) with retarded boundary conditions yields the term in the generating functional (effective action) of real-time amplitudes which is linear in the Keldysh A_a field:

$$\begin{aligned} \Gamma^{(1)} &= m_D^2 \int \frac{d\Omega_v}{4\pi} \int d^4 X v \cdot A_a \frac{1}{v \cdot D[A_r]} \mathbf{v} \cdot \mathbf{E}[A_r] \\ &\equiv m_D^2 \int \frac{d\Omega_v}{4\pi} \int d^4 X \int_0^\infty d\tau v_\mu A_a^{\mu a}(X) U^{ab}(X, X - v\tau) [A_r] v^i E^{ib}[A_r](X - v\tau), \end{aligned} \quad (4.3)$$

where U^{ab} stands for an adjoint Wilson line along the hard particle trajectories. Here we have explicitly performed the radial integration in (4.1), leaving only the integration over the angle \mathbf{v} of the hard particles; in a generic Yang-Mill theory with N_F Dirac fermions and N_S complex scalars, the degree of freedom counts add up to:

$$m_D^2 = \frac{g^2 T^2}{3} [C_A + N_F T_F + N_S T_S], \quad (4.4)$$

where $C_A = N_c$ and $T_F = T_S = \frac{1}{2}$ in $SU(N_c)$ gauge theory with matter in the fundamental representation.

We find (4.3) rather physically transparent compared to its Euclidean counterpart [17] [18], however compact the latter might be. The equivalence between the analytic continuation of the vertex functions derived from (4.3) and the standard Euclidean ones can be verified from the explicit expressions for the induced current $\delta\Gamma_{\text{Euclidean}}/\delta A$ given in [18]. It is a rather nontrivial, although necessary, property of these functions that they become symmetrical in all of their arguments (including the a leg) when the boundary conditions are made symmetrical, by analytically continuing the momenta to imaginary frequencies. However, it is this very

asymmetry between the a leg (“induced current”) and the r legs (“external fields”) of the fully retarded vertex functions, at physical values of the momenta, which makes the generating functional (4.3) so simple. We describe the Fourier space amplitudes derived from (4.3) in more detail, in section 5.

4.2 HTLs with two a indices

We now compute the hard thermal loops with two external a indices, beginning with the aa self-energy. The relevant Feynman diagrams are shown in Fig. 3 (a)-(c); the propagators in these diagrams are most conveniently added together under the integration sign:

$$G_{rr}(Q)G_{rr}(R) + \frac{1}{4}G_R(Q)G_R(R) + \frac{1}{4}G_A(Q)G_A(R) \simeq \frac{1}{2} [G^>(Q)G^>(R) + G^<(Q)G^<(R)] , \quad (4.5)$$

the equality holding up to analytic terms which integrate to zero such as $G_R(Q)G_A(R)$ (“closed loops of retarded propagators”), which we have subtracted in passing to the right-hand side. Here the propagators $G^{>,<}$ denote the Wightman (unordered) two-point functions, and we have employed the identities $G_R - G_A = G^> - G^<$, $G_{rr} = \frac{1}{2}(G^> + G^<)$. Equation (4.5) states that the aa self-energy is the average of the two Wightman self-energies, a cutting pattern which we graphically represent with two parallel lines, as in Fig. 3 (d), in analogy with our notation for the G_{rr} propagator. Evaluating the loop for a complex scalar field, for definiteness, yields:

$$\begin{aligned} i\Gamma_{aa\mu\nu}^{ab}(P) &= -g^2 \text{Tr}_r \left[t_r^a t_r^b \right] \int \frac{d^4 Q}{(2\pi)^4} (2Q + P)_\mu (2Q + P)_\nu \frac{G^>(Q)G^>(R) + G^<(Q)G^<(R)}{2} \\ &\approx -g^2 \sum_{\text{DOF}} \text{Tr}_r \left[t_r^a t_r^b \right] \int \frac{d^3 q}{(2\pi)^3} 2\pi \delta(v \cdot P) v_\mu v_\nu n_B(q) (1 + n_B(q)) , \end{aligned} \quad (4.6)$$

where on the second line we have used $P \ll Q$ since the integral is saturated for $Q \sim T$. We see that the calculation of this self-energy is relatively simple, compared to the corresponding retarded HTL self-energy: since no $\mathcal{O}(g)$ cancellation occurs, all $P \ll Q$ approximations can be applied directly. Particles of different spins yield similar contributions (up to $\mathcal{O}(g)$ corrections), and one gets the same degree of freedom count as in (4.1). The self-energy (4.6) could also be obtained by means of the KMS (fluctuation-dissipation) relation, which relates the aa HTL self-energy to T/p^0 times the discontinuity of the retarded HTL self-energy.

Equation (4.6) has a rather straightforward physical interpretation: the double cut in diagram (d) describes thermodynamical equal-time fluctuations,

$$\langle n^a(\mathbf{x}, \mathbf{q}) n^b(\mathbf{x}', \mathbf{q}') \rangle = \text{Tr}_r \left[t_r^a t_r^b \right] \delta^3(\mathbf{x} - \mathbf{x}') (2\pi)^3 \delta^3(\mathbf{q} - \mathbf{q}') n_B(q) (1 + n_B(q)) , \quad (4.7)$$

affecting the distribution functions which appear in (4.1). Expression (4.6) is precisely $(i)^2$ times the Fourier transform of the unequal time correlator derived from (4.7), by means of ballistic propagation $v \cdot \partial n^a(X, \mathbf{q}) = 0$. Considerations of gauge invariance immediately

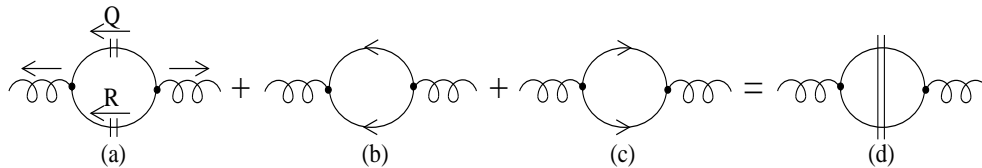


Figure 3: (a)-(c): Diagrams contributing to the aa gluon self-energy, with momentum assignments displayed on the first diagram. (d) The sum of the three preceding diagrams. The double cut represents the average of the Wightman cuts in the two direction.

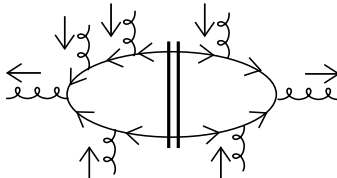


Figure 4: The most general form of diagram contributing to gluon HTLs with two a indices but many r indices. Diagrams with four point vertices are subleading. The double-cut has the same meaning as in Fig. 3.

suggest that to obtain the fluctuation functions with external r gauge fields, one should merely substitute this free ballistic propagation with a gauge-covariant one, $v \cdot D[A_r]n^a(X, \mathbf{q}) = 0$.

Not surprisingly, this expectation is borne out by explicit calculations. This is especially obvious to see if one begins with a reorganization of the r/a structure of the relevant diagrams, in a way analogous to (4.5) above. Indeed, although a direct application of the rules of the Schwinger-Keldysh formalism would yield diagrams which correspond to inserting the external r fields onto the diagrams (a)-(c) of Fig. 3, it can be proved that their sum is equivalent to what is obtained by inserting the r fields directly onto the simpler diagram (d): all of the diagrams thus obtained contain two cut (Wightman) propagators, which appear at the smallest time, as illustrated in Fig. 4. Making all small P approximations to the propagators and vertices in these diagrams amounts to taking the propagation of the hard particles to be eikonal, e.g. given by Wilson lines along their classical trajectories, justifying the procedure mentioned in the preceding paragraph of replacing $v \cdot \partial$ with $v \cdot D[A_r]$.

Thus, upon performing the radial integration in (4.6), we obtain the generating functional for vertex functions with two a indices (with m_D^2 as in (4.4)):

$$\Gamma^{(2)} = \frac{m_D^2 iT}{2} \int \frac{d\Omega_v}{4\pi} \int d^4X \int_{-\infty}^{\infty} d\tau v_\mu A_a^{\mu a}(X) U^{ab}(X, X - v\tau) [A_r] v_\nu A_a^{\nu b}(X - v\tau) \quad (4.8)$$

Although it should be rather obvious, from their manifest gauge-covariance, that the vertex functions obtained from (4.3) and (4.8) obey a large class of Ward identities, we remark that the full HTL effective action $\Gamma^{(1)} + \Gamma^{(2)}$ is not strictly invariant under the whole

only one external a index, enters the calculation of amplitudes with two external a indices (in which it appears exactly once). By $(v \cdot P^-)$ we mean

$$\frac{1}{v \cdot P^-} \equiv \frac{1}{v \cdot P - i\epsilon}. \quad (5.2)$$

The effective propagators and interaction vertices of Fig. 5 are to be used in building Feynman diagrams according to the standard rules of the r/a formalism; the objects (a)-(c) correspond to ar interaction vertices, the propagator (e) is a retarded (ra) propagator and (f) represents an rr propagator. The interaction vertex (d) carries arr indices and is the only such interaction vertex in this theory; there is no three-point vertex involving an a gluon. In practice the self-energies on soft gluon lines must be resummed; when this resummation is performed the insertion (a) should be ignored, as well as all diagrams in which only two gluons connect to a double line. We have not explicitly shown the tree interaction vertices between soft gluons, although these are of the same order as the HTL ones and must be included in the effective theory.

The double lines in our graphical rules may be thought of as two-particle states (alternatively, one-particle density matrices): in general, by “opening up” these double lines the one-loop diagrams considered in section 4 are recovered, or more precisely, specific sums of these diagrams. As we comment on below, these graphical rules represent purely classical plasma physics.

5.1 An example

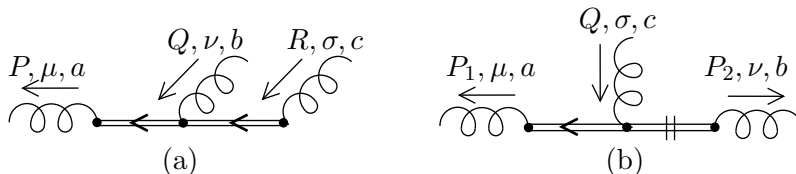


Figure 6: Effective Feynman diagrams contributing to HTLs with three external legs, up to permutations. (a) HTLs with one a index. HTL. (b) HTLs with two a indices.

As an example of the application of these rules, we evaluate the three-point HTLs. The relevant diagrams are shown in Fig. 6, and upon adding their permutations, the application of the rules produces:

$$\Gamma_{arr}{}^{abc}(P; Q, R) = im_D^2 f^{abc} \int \frac{d\Omega_v}{4\pi} \frac{v_\mu v_\nu v_\sigma}{v \cdot P^-} \left[\frac{r^0}{v \cdot R^-} - \frac{q^0}{v \cdot Q^-} \right], \quad (5.3)$$

$$\Gamma_{aar}{}^{abc}(P_1, P_2; Q) = m_D^2 T f^{abc} \int \frac{d\Omega_v}{4\pi} \frac{v_\mu v_\nu v_\sigma}{v \cdot Q^-} [2\pi\delta(v \cdot P_2) - 2\pi\delta(v \cdot P_1)]. \quad (5.4)$$

Our notation for Γ , which corresponds to $(-i)$ times the amputated Feynman diagrams themselves, is that the momenta written before the semicolon are outgoing and the others are incoming. In particular, momentum conservation implies $P = Q + R$ and $P_1 + P_2 = Q$ (see

Fig. 6). Our result for the retarded three-point function agrees with the standard one; we have also verified the four-point function. Our result (5.4) for the vertex function with two a indices agrees with that of [16], Eq. (III.18e) (one must take into account that their Γ_{RRA} function is $2i$ times our Γ_{aar} , that their momenta are incoming, and their metric is different from ours.)

6. Discussion

In this paper we have given the generating functional for all hard thermal loops in the real-time formalism, (4.3) and (4.8). The form of these amplitudes is deceptively simple: a classical plasma physicist, instructed of the fact that nonabelian charges tend to precess in the presence of a gauge field, would have known enough to simply write them down decades ago. Indeed, we find that there are only two kinds of HTL amplitudes: amplitudes with only one external Keldysh a index, which describe the (nonlinear) polarizability of a medium of nonabelian point-charges, and amplitudes with two external Keldysh a indices, which represent current-current correlations in such a medium. What we think is most interesting about our findings, is the fact that these functions form the complete real-time HTL theory. The essential reason for this, discussed in section 3, is that the Keldysh a (“difference”) fields, compared to the Keldysh r (“average”) fields, are unable to take advantage of the large occupation numbers of the soft gauge fields, hence diagrams containing more Keldysh a indices naturally tend to be subleading. Incidentally, loop amplitudes with more than two external a indices are actually soft-dominated, not hard-dominated.

We have given simple effective Feynman rules, in section 5, which generate the hard thermal loop amplitudes; physically these rules are nothing but a graphical representation of the nonabelian Vlasov equations (see e.g. [22] or the review [21]). Diagrams not involving the cut propagator (f) of Fig. 5, account for the classically induced current (5.1) due to a background mean field, and whenever this (f) propagator appears, its role is to account for the Gaussian fluctuations (4.7) of the particle distribution functions (corresponding to fluctuations of the “ W ” fields in the language of [21]). The importance of such Gaussian fluctuations was discussed previously in the context of the hot electroweak theory (see [23]); the analysis of the HTL theory given in [24], of which we became aware after this work was completed, bears much similarity with ours.

Our findings extend in a straightforward manner to nonequilibrium setups: one should simply replace the distribution functions in (4.1) and (4.7) by their time-dependent expressions. As was argued for in great detail in [25], this procedure will be correct provided the naive criterion for it to make sense is satisfied: the distribution functions of the particles should be slowly varying on the length and time scale set by the “soft” gauge fields (those for which the HTL effects become important). Also, the perturbation theory employed here should make sense: this requires a separation of scales between the “soft” scale and the momenta of the particles which dominate the integrals (4.1) and (4.7) (in this paper this separation is $gT \ll T$).

Even though the close relationship between the HTL theory and classical plasma physics has been widely recognized for a long time, it was not clear, at least to the author, how this understanding could be exploited in the context of the next-to-leading order calculation of dynamical quantities like the ones listed in the introduction. The difficulty is that at leading order one has to deal not only with soft, classical physics, but also with some truly quantum physics. This is the context in which we believe a systematic, *a priori* fully quantum mechanical approach, starting from the Feynman diagrams of the real-time formalism, can be most useful.

7. Acknowledgements

This work was supported in part by the Natural Sciences and Engineering Research Council of Canada.

References

- [1] J. Adams *et al.* [STAR Collaboration], Nucl. Phys. A **757**, 102 (2005) [arXiv:nucl-ex/0501009].
- [2] E. Braaten and A. Nieto, Phys. Rev. Lett. **76**, 1417 (1996) [arXiv:hep-ph/9508406].
- [3] R. Baier, H. Nakkagawa, A. Niegawa and K. Redlich, Z. Phys. C **53**, 433 (1992).
- [4] J. Kapusta, P. Lichard and D. Seibert, Phys. Rev. D **44**, 2774 (1991) [Erratum-*ibid.* D **47**, 4171 (1991)].
- [5] P. Aurenche, F. Gelis, R. Kobes and H. Zaraket, Phys. Rev. D **58**, 085003 (1998) [arXiv:hep-ph/9804224].
- [6] P. Arnold, G. D. Moore and L. G. Yaffe, JHEP **0206**, 030 (2002) [arXiv:hep-ph/0204343].
- [7] R. Baier, Y. L. Dokshitzer, A. H. Mueller, S. Peigne and D. Schiff, Nucl. Phys. B **483**, 291 (1997) [arXiv:hep-ph/9607355].
- [8] B. Svetitsky, Phys. Rev. D **37**, 2484 (1988).
- [9] E. Braaten and M. H. Thoma, Phys. Rev. D **44**, 2625 (1991); Phys. Rev. D **44**, 1298 (1991).
- [10] P. Arnold, G. D. Moore and L. G. Yaffe, JHEP **0305**, 051 (2003) [arXiv:hep-ph/0302165].
- [11] E. Braaten and R. D. Pisarski, Nucl. Phys. B **337**, 569 (1990).
- [12] S. Caron-Huot and G. D. Moore, arXiv:0708.4232 [hep-ph]; S. Caron-Huot and G. D. Moore, in preparation.
- [13] K. C. Chou, Z. B. Su, B. L. Hao and L. Yu, Phys. Rept. **118**, 1 (1985).
- [14] T. S. Evans, Nucl. Phys. B **374**, 340 (1992).
- [15] J. Frenkel and J. C. Taylor, Nucl. Phys. B **334**, 199 (1990).
- [16] Y. Fueki, H. Nakkagawa, H. Yokota and K. Yoshida, Prog. Theor. Phys. **107**, 759 (2002) [arXiv:hep-ph/0111275].
- [17] E. Braaten and R. D. Pisarski, Phys. Rev. D **45**, 1827 (1992).

- [18] J. C. Taylor and S. M. H. Wong, Nucl. Phys. B **346**, 115 (1990).
- [19] J. P. Blaizot and E. Iancu, Phys. Rev. Lett. **70**, 3376 (1993) [arXiv:hep-ph/9301236].
- [20] R. Jackiw and V. P. Nair, Phys. Rev. D **48**, 4991 (1993) [arXiv:hep-ph/9305241].
- [21] J. P. Blaizot and E. Iancu, Phys. Rept. **359**, 355 (2002) [arXiv:hep-ph/0101103].
- [22] P. F. Kelly, Q. Liu, C. Lucchesi and C. Manuel, Phys. Rev. D **50**, 4209 (1994)
- [23] P. Huet and D. T. Son, Phys. Lett. B **393**, 94 (1997) [arXiv:hep-ph/9610259].
- [24] D. T. Son, arXiv:hep-ph/9707351.
- [25] M. E. Carrington, D. f. Hou and M. H. Thoma, Eur. Phys. J. C **7**, 347 (1999) [arXiv:hep-ph/9708363].